

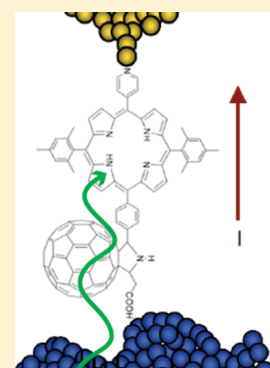
Optical Modulation of Molecular Conductance

Shreya Battacharyya,^{†,§} Ashley Kibel,^{†,§} Gerdenis Kodis,[†] Paul A. Liddell,[†] Miguel Gervaldo,[†] Devens Gust,[†] and Stuart Lindsay^{*,†,‡,§}[†]Department of Chemistry and Biochemistry, [‡]Department of Physics, [§]Biodesign Institute, Arizona State University, Tempe, Arizona 85287, United States

S Supporting Information

ABSTRACT: A novel scanning probe microscope stage permits break junction measurements of single molecule conductance while the molecules are illuminated with visible light. We studied a porphyrin-fullerene dyad molecule designed to form a charge separated state on illumination. A significant fraction of illuminated molecules become more conductive, returning to a lower conductance in the dark, suggesting the formation of a long-lived charge separated state on the indium–tin oxide surface. Transient absorption spectra of these molecular layers are consistent with formation of a long-lived charge separated state, a finding with implications for the design of molecular photovoltaic devices.

KEYWORDS: Molecular electronics, optoelectronics, molecular photovoltaics, charge-separated states, indium tin oxide



Natural photosynthetic reaction centers serve as inspiration for construction of solar energy conversion devices that generate long-lived charge separated states by photoinduced electron transfer on illumination.^{1,2} Much is known about the solution properties of such molecules, but it is much more difficult to study their properties when the molecules are in contact with electrode materials. Single molecule measurements can provide information of this kind and also shed light on the heterogeneity of the interface. Scanning probe microscope studies of the electronic properties of optically activated molecules have been limited to photochromes that can be switched between long-lived conformational states^{3,4} because the lifetimes of the excited states of nonphotochromic chromophores are generally too short for probing the excited state population by STM methods. Ho has used pulsed laser illumination to detect transient charging of a molecule on a thin oxide film.⁵ The use of metal electrodes⁶ limits optical access and leads to quenching of the excited state. Tao et al. used a probe coated with indium–tin oxide (ITO) on a transparent ITO substrate to demonstrate that single-molecule conductance can be measured on this surface, but the study was limited to n-alkanes that do not absorb visible light.⁷ Here, we show that single molecule break junction measurements can be made with ITO–gold junctions with molecules that absorb light, allowing the effects of illumination on molecular junctions to be studied directly. We used a molecular dyad consisting of a porphyrin chromophore and a C₆₀ electron acceptor,⁸ a complex that gives rise to a charge-separated state when illuminated with visible light. The lifetime of the charge-separated state is on the order of nanoseconds in solution, so the fraction of molecules in the excited state at the time of a conductance measurement should be vanishingly small.

Nonetheless, strong, reversible effects were observed when the molecules were illuminated.

An Agilent (Chander, AZ) PicoSPM equipped with an STM scanner utilizing a 1 nA/V current preamplifier was fitted with a custom sample stage that allowed optical access to the sample from below (Figure 1A). An ITO substrate was illuminated using an Ar/Kr laser (CVI Melles-Griot, Albuquerque, NM) operating at 520 nm and focused to a 0.48 mm diameter spot on the sample. The beam was directed onto the SPM antivibration stage via a single-mode optical fiber and transferred into the microscope's environmental chamber through a window. An adjustable fiber collimator (Thor Laboratories, Newton, NJ) mounted in a five-axis lens positioner (Newport Corporation, Irvine, CA) was used for final alignment. A neutral density filter was placed in the beam path for power adjustment and the illumination was switched on and off by means of a remotely actuated shutter (Thor Laboratories, Newton, NJ). The environmental chamber was purged with Ar that had been chemically scrubbed to remove oxygen. The sample was mounted in liquid cell under freshly distilled mesitylene that had been sparged with argon.

ITO presents a poorly defined surface, both chemically and physically (Figure S1 in Supporting Information). Nonetheless, good conductance histograms have been obtained for carboxylate terminated alkanes on ITO.⁷ In the present work, we used molecules terminated at one end with a carboxylate, and at the other with a pyridyl group (Figure 2) with the expectation that the carboxylate would adhere to the ITO and the pyridyl moiety to the gold probe (Figure 1B). We tested this scheme using

Received: March 23, 2011

Revised: May 24, 2011

Published: June 09, 2011

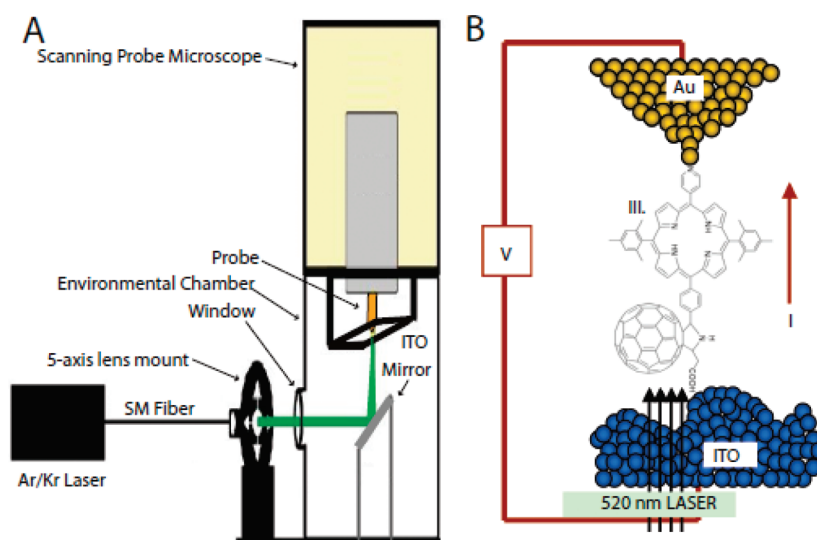


Figure 1. Single-molecule break junction measurements with optical illumination. (A) A monolayer of molecules on an ITO substrate is illuminated from below by a laser beam coupled to the STM by an optical fiber. A gold probe is pushed into and retracted from the substrate from above. (B) The expected bonding geometry of a porphyrin-C60 dyad molecule in the gold–ITO tunnel junction. A carboxylate interacts with ITO and a pyridyl moiety binds to the gold probe.

(pyridine-4-yl)propionic acid, an *n*-alkane with the same terminations (**I** in Figure 2). We found clear signatures of single molecule trapping in the break junction with corresponding features in the conductance histograms (Supporting Information Figure S7). In order to test the validity of this result, we examined molecules that were thiol-terminated at one end, for which a series of alkane chain lengths were available (mercapto-propionic acid ($N = 3$), mercaptohexonic acid ($N = 6$) and mercapto-octonic acid ($N = 8$)). The decay constant ($\beta = 0.88$ per CH_2 group, Supporting Information Figure S4) deduced from these measurements was in good agreement with previously reported data for *n*-alkanes, which varies between 1.0 to 0.8 per $-\text{CH}_2$ group.^{7,9} The measured conductance for (pyridine-4-yl)propionic acid is below the value for $N = 3$ (as expected because of the three extra carbons in a path through the pyridyl ring) but above the value for $N = 6$ (as expected because of the conjugation of the pyridyl ring). Thus, we conclude that the pyridyl and carboxylate anchoring groups enable break-junction measurements in a gold–ITO tunnel junction.

To test for optical-modulation of molecular conductance, we synthesized a porphyrin-C₆₀ dyad bearing a pyridyl group attached to the porphyrin and a carboxylate attached to the C₆₀ (**III** in Figure 2). Full details of the synthesis and characterization are given in the Supporting Information. Monolayers of these dyads were made by immersing oxygen-plasma cleaned glass substrates (coated with ITO on one side) in a 5 μM solution of the porphyrin-fullerene dyad in mesitylene overnight, rinsing them with mesitylene and drying them in a stream of nitrogen. The molecular adlayer on the glass side of the substrate was washed off with dichloromethane for optical spectroscopy. Spectroscopic measurements showed that the absorbance of the slides increased by 0.052 at the Soret band wavelength (430 nm) after formation of the molecular adlayer (Figure 3A). The extinction coefficient of the dyad in dichloromethane solution, ϵ , is 507 770 (mol/liter)⁻¹ cm⁻¹ at 419 nm. The Soret bandwidth in the film (Figure 3A) is 2.7 times that in solution, so ϵ in the film $\sim 190\,000$ (mol/liter)⁻¹ cm⁻¹. From this value, we calculate the number of molecules in the film on

one side of the substrate to be 1.6×10^{14} molecules/cm². Molecular mechanics modeling shows that a densely packed monolayer could accommodate $\sim 0.6 \times 10^{14}$ molecules/cm² but, given the roughness of the ITO surface (Supporting Information Figure S1) these numbers are consistent with the formation of a monolayer. This conclusion is supported by angle-resolved XPS (Supporting Information Figure S2) that yielded an adlayer thickness of 1.95 nm, consistent with a slightly tilted monolayer.

Repeated STM break junctions were formed using custom Labview software controlling a National Instruments data acquisition device (NI USB-6221) as previously described.¹⁰ The surface was first surveyed by STM imaging in order to assess the quality of the surface and probe (Supporting Information Figure S1). If the surface was found to be reasonably flat, control was passed to the Labview program where the probe was approached to a preset current value (usually to 10 nA at -0.4 V bias) and then retracted at a rate of 20–40 nm/s while current was recorded on a Tektronix TDS 2004B oscilloscope, along with piezo voltage, bias and optical shutter voltage. A selection of typical conductance versus time decay curves showing current plateaus are given in Figure 3B. These data were displayed as a histogram as described by Chen et al.¹⁰ Chen's procedure uses changes in slope to identify and count plateaus (as illustrated by the exponential fits on each side of the plateaus in Figure 3B). This approach eliminates a background owing to the exponentially decaying current, but produces a feature near zero conductance owing to the assignment of a small slope at the end of the decay as a "plateau" by the analysis program. We show histograms compiled from all the current data in the Supporting Information (Figure S5). When all the data is used, the plateaus produce peaks because of the additional current data points they generate. The single molecule conductance peak is still visible in Supporting Information Figure S5, sitting on top of the background produced by the exponential decay. When no molecules were present (control data inset in Figure 3C) only the feature near zero current was observed in the distribution. Samples coated with monolayers of the dyad **III** showed a conductance peak at 2.5 nS (arrow in Figure 3C).

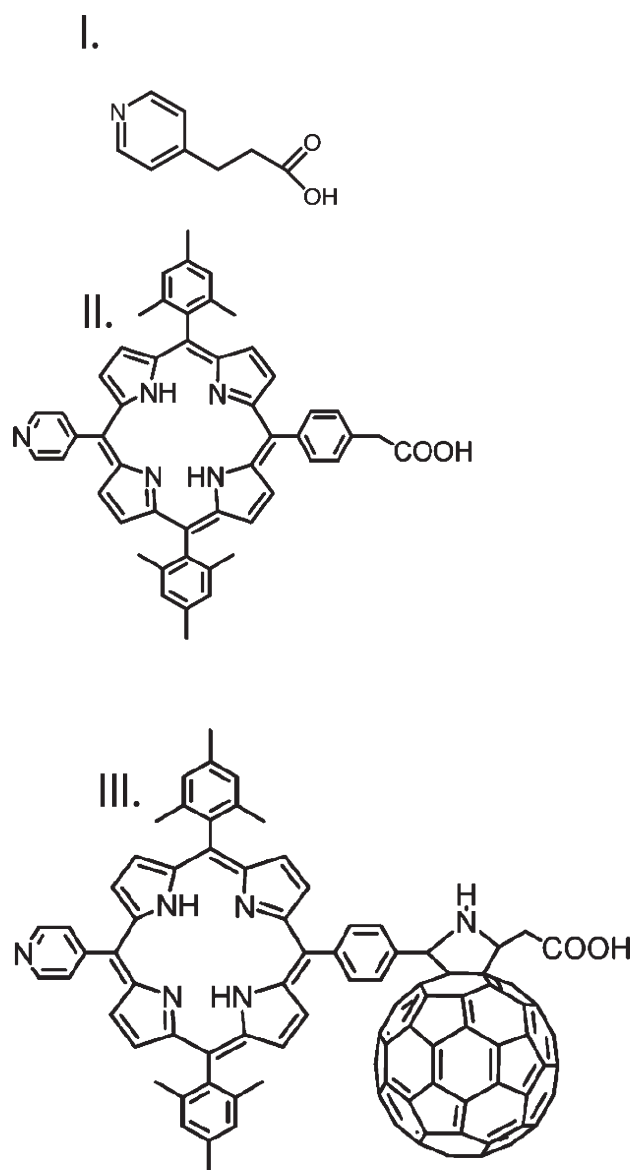


Figure 2. Molecules used in this study: I, 3-(pyridine-4-yl)propionic acid; II, porphyrin; and III, porphyrin- C_{60} dyad, all functionalized with carboxylate and pyridyl moieties.

When the sample was illuminated at 520 nm at high power densities, we found that conductance values decayed with exposure time, indicative of photo damage. We then collected data from the same spot on the sample, alternating between dark and illuminated conditions in ten minute intervals, adjusting the power density until the data became reversible (at or below 200 mW/cm^2 , Figure 4). Figure 3C,D shows reversible data aggregated from 5 ten minute blocks of dark recordings (Figure 3C) and 5 ten minute blocks of light recordings (Figure 3D) taken at 200 mW/cm^2 . Inspection of Figure 3D shows that a new, high conductance feature appears at 4.3 nS (P2) when the sample is illuminated. This additional conductance peak was not found in a sample lacking a chromophore (I, 3-(pyridine-4-yl)propionic acid, Supporting Information Figure S7) nor in a bare ITO sample when illuminated (inset, Figure 3D). It was not present (Supporting Information Figure S8) in a sample consisting of the porphyrin chromophore alone (II Figure 2). It is interesting to

note that the conductance of III is only slightly lower than that of II despite the significantly greater length of molecule III.

We estimated the number of molecules in the high conductance state by fitting both peaks (P1 and P2) with Gaussians, taking the relative number of molecules in each state to be proportional to the area of the corresponding Gaussian. The fraction of molecules in the high conductance state increased linearly with power density up to a maximum of 50% at the largest power density that gave reversible results (Figure 4).

The high conductance state is not a result of irreversible photochemistry. It also cannot be a consequence of photogenerated current. The absorption cross section of these chromophores at 520 nm is $\sim 1 \text{ \AA}^2$ and 200 mW/cm^2 corresponds to a photon density of 47 photons $\text{\AA}^{-2} \text{ s}^{-1}$ that in turn gives ~ 50 photons absorbed per molecule per second. Even if several molecules (perhaps up to three under a 1 nm radius probe) contribute photocurrent, it could not exceed a small fraction of a femtoampere. The lifetime of the charge separated state as measured in solution (~ 3 ns, measured for a similar dyad¹¹) is much too short to result in excitation of 50% of the population because the average molecule would be in the charge separated state for only ~ 3 ns, ~ 50 times a second. An enhanced conductance is often a consequence of charging a molecule.^{10,12,13} Is it possible that the lifetime of the charge-separated state is greatly enhanced by charge transfer to the ITO surface? We set out to find evidence of a long-lived charge-separated state using optical transient absorption measurements.

We first performed fluorescence decay studies on films of II and III on an ITO-coated glass electrode in air and on a solution of III in mesitylene solution with excitation into the Soret region at 420 nm (< 10 pJ per pulse). For the films, the fluorescence signal was doubled by stacking two slides together, each functionalized only on the ITO-coated side. The decay kinetics at 720 nm (not shown) of III in mesitylene solution were fitted with exponential decays having lifetimes of 143 ps (89%), 1.44 ns (10%), and 10.26 ns (1%), $\chi^2 = 1.05$. The 143 ps lifetime is associated with singlet-singlet energy transfer from porphyrin to fullerene while 1.44 and 10.26 ns are characteristic lifetimes of singlet excited state of this kind of fullerene and porphyrin, respectively. Figure 5A shows fluorescence decay kinetics for films of III (black circles) and for films of II (blue squares). The decay kinetics at 660 nm were fitted with exponential decays having lifetimes of 36 ps (90%), 550 ps (6%), 5.14 ns (4%), $\chi^2 = 1.05$ for III, and 95 ps (53%), 360 ps (28%), 1.29 ns (16%), 5.75 ns (3%), $\chi^2 = 1.01$ for II. The decay kinetics of film III at 720 nm (Supporting Information Figure S12) were fitted with exponential decays having lifetimes of 36 ps (83%), 450 ps (13%), 4.33 ns (4%), $\chi^2 = 1.03$.

The film of porphyrin II shows nonexponential fluorescence decay reflecting exciton migration from higher- to lower-energy states that result from heterogeneity of the molecular film. The greatly shortened excited-state lifetimes in film II relative to that of II in solution (10.26 ns) reflect efficient excited-state quenching processes in the molecular film sample. In the case of film III, the lifetime of the vast majority of the porphyrin first excited singlet states is ~ 36 ps, which is much shorter than the lifetimes of these states in film II or in mesitylene solution. This lifetime is similar to the porphyrin excited state lifetime in similar dyads in polar solvents, where the quenching is due to photoinduced electron transfer to the fullerene to yield $P^{*+} - C_{60}^{\bullet-}$.¹¹ The 450 ps component may be associated with the decay of the fullerene excited state to form the same charge separated state.

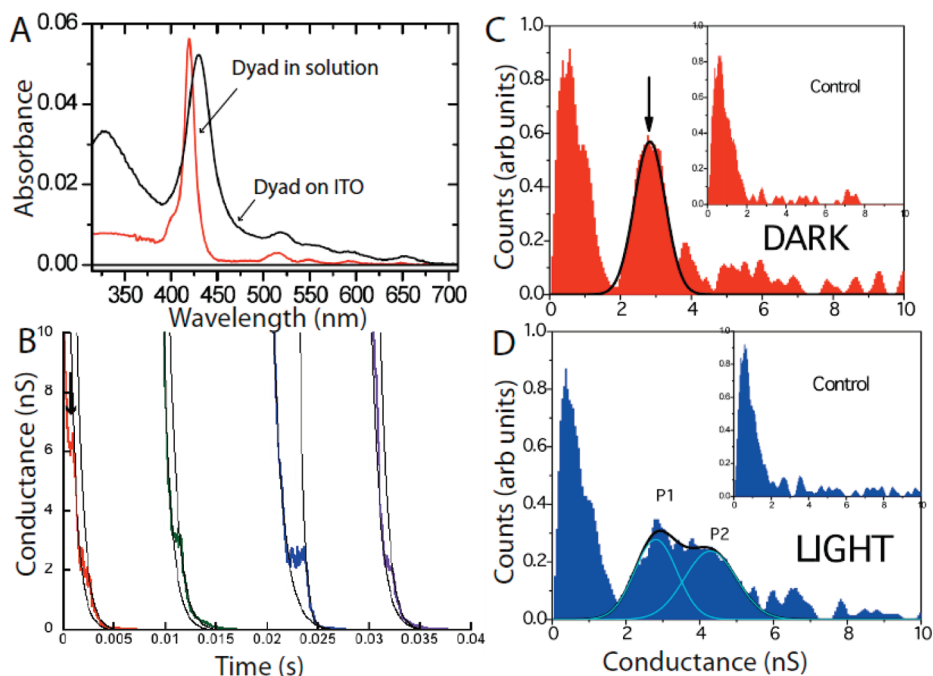


Figure 3. Conductance of porphyrin- C_{60} dyads under illumination. (A) Absorption spectra of the dyad in mesitylene solution (red) and on the ITO substrate (black). The Soret band appears at ~ 430 nm, and the four Q bands at ~ 519 , 554, 593, and 652 nm. (B) Typical conductance versus time traces as the probe is retracted for the dyad in the dark at a bias of -0.4 V. Black lines are exponentials fitted to each side of the plateau showing how a single exponential plus a noise spike would not fit the decays. The arrow by the red curve points to a second conductance plateau. (C) Distribution of conductances for the dyad in the dark. The peak near 0 nS is seen on a bare ITO substrate (inset) and is a spurious output of the algorithm that identified plateaus in the conductance decay curves (Supporting Information). The feature at 2.5 nS (arrow) is only observed when a monolayer of the dyad molecules is present (solid line is a Gaussian fit). The smaller features at higher conductance are not reproducible from run to run (Supporting Information Figure S9). (D) Distribution of conductances for the dyad illuminated at 520 nm ($200 \text{ mW}/\text{cm}^2$). The current distributions were converted to conductance using the probe bias of 0.4 V. Illumination generates a second conductance peak (P2) at 4.3 nS. This feature is reversible, disappearing when the sample is returned to dark conditions. Black line is a fit to the sum of two Gaussians (green curves). Inset shows the conductance distribution for bare ITO under illumination. Here again, the peak near zero conductance is an artifact of the program that locates plateaus in the data. Histogram counts were normalized so that the highest feature was approximately unity.

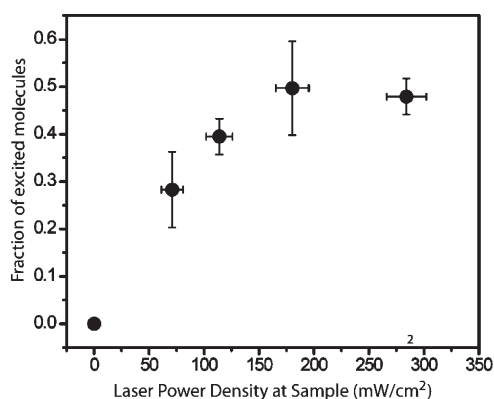


Figure 4. Fraction of molecules in the excited (P2) state as a function of laser power density. The number of molecules in each state is taken to be proportional to the product of the height and width of the Gaussian fits. The number of molecules in the high conductance (P2) state falls once the power density exceeds $200 \text{ mW}/\text{cm}^2$, a power density above which conductance changes become irreversible.

Transient absorbance measurements required a stack of six sandwiched ITO substrates (coated on the ITO side only). Each molecular adlayer was separated from its neighboring slide by a small air gap in order to minimize optical interference. Transient absorption pump–probe measurements were made

with excitation at 520 nm (~ 90 nJ, ~ 100 fs pulse) to minimize excitation of the fullerene and ITO, and also at 430 nm near the Soret maximum (~ 2 mJ, 5 ns pulse). Detection was at 550–880 nm (see transient spectra in the inset, Figure 5C), a spectral region in which most of the induced absorbance is attributed to porphyrin radical cations (polarons and CT excitons), although some excited-state absorbance, ground-state bleaching, and stimulated emission due to Frenkel excitons may also be present (Figure 5B,C). Although the decays are likely nonexponential (Figure 5B,C and Supporting Information Figures S13 and S14) they can be fitted with five exponential components: 40 ps, 290 ps, 1.95 ns, 600 ns, and 14 μs . The last two components are from nanosecond transient absorption kinetics. These longer time constants were not resolved in the femtoseconds–picoseconds experiments). The 40 ps lifetime is similar to the fluorescence decay lifetime (36 ps) and appears as a rise of induced absorbance or decay of stimulated emission in kinetics around 700 nm (transient spectra in the Figure 5C inset) and may be associated with formation of $P^{+\bullet}-C_{60}^{\bullet-}$ charge-separated states (CT excitons). The 290 ps and 1.95 ns lifetimes are similar to the recombination times of $P^{+\bullet}-C_{60}^{\bullet-}$ charge-separated state (CT excitons) observed in similar dyad components of polymers.¹⁴ The short lifetimes of the excited singlet states (fluorescence results above) preclude significant triplet production by intersystem crossing. Thus overall results are consistent with very fast decay of the porphyrin first excited

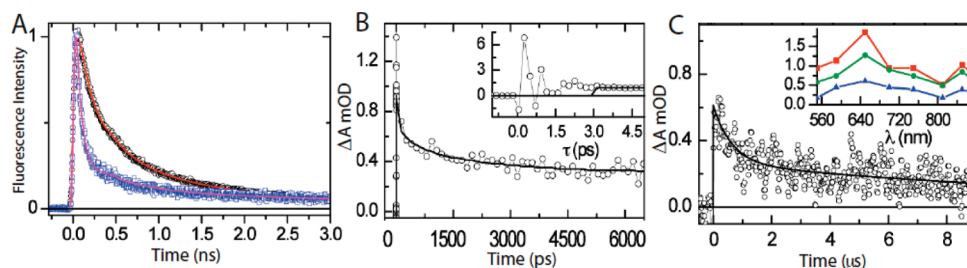


Figure 5. (A) Time-resolved fluorescence data for monolayer films of **II** (black circles) and **III** (blue squares) on ITO-coated glass, following excitation at 420 nm with a ca. 100 fs laser pulse. The solid lines are exponential decays convoluted with the instrument response function. (B) Transient absorption kinetics at 850 nm for a stack of six ITO-coated glass plates covered with films of dyad **III** following excitation at 520 nm with 100 fs pulses. Inset shows transient absorption kinetics with ~ 1.5 THz oscillations due to longitudinal hypersonic waves at earlier time delays. (C) Transient absorption kinetics at 700 nm for a similar stack of plates with films of dyad **III** following excitation at 430 nm with 5 ns pulses. The solid lines are multiple exponential decays. The inset shows transient absorption spectra at 3 ps (red squares), 10 ps (green circles), and 2 ns (blue triangles) obtained with excitation at 520 nm with 100 fs pulses.

singlet state by photoinduced electron transfer to yield molecular $P^{*+}-C_{60}^{\bullet-}$ charge-separated states (CT excitons), which migrate and decay over a variety of time scales forming long living (at least many microseconds) polarons. These long-lived states are unique to the solid-state sample of **III** and may therefore be responsible for the large fraction of molecules found to be in a high conductance state when the sample is illuminated.

Similar experiments were carried out with films of porphyrin **II** and the bare ITO on glass substrate. No measurable transient absorption signal at 700 nm was observed for either sample with excitation at 430 nm using 5 ns laser pulses. On the basis of spectroscopic and cyclic voltammetric measurements (Supporting Information Figure S9), the energy of the porphyrin first excited singlet state in the film is 1.9 eV above the ground state, and the energies of the $P^{*+}-P^{*-}$ and $P^{*+}-C_{60}^{\bullet-}$ charge-separated states are 2.32 and 1.77 eV, respectively. Thus, although photoinduced electron transfer in **III** is thermodynamically favorable, photoinduced electron transfer to form $P^{*+}-P^{*-}$ in porphyrin **II** film would be very endergonic and dissociation of singlet excited states (Frenkel excitons) to form polarons is most likely not possible.

In summary, we find a significant fraction of porphyrin- C_{60} dyad molecules under optical illumination remain in an enhanced conductance state for long periods, allowing their observation using scanning tunneling microscopy. Recombination to the ground state occurs without chemical decomposition of the molecule, and the fraction of the population in the enhanced conductance state is proportional to the illumination intensity, up to the threshold for photodamage. Transient absorption spectra show that a long-lived polaronic state is formed in molecular films of this dyad on ITO but not in solution or in films of the porphyrin alone. Although the nature of these states is unknown, it is reasonable to conclude on the basis of the experiments that absorption of light leads to formation of $P^{*+}-C_{60}^{\bullet-}$ by photoinduced electron transfer, and that the resulting charges migrate away from the site of initial electron transfer, via hopping to adjacent molecules and/or migration into the ITO conductive substrate. Recombination of these separated charges is slow, allowing the state to be observed in conductance measurements. This unexpected interaction with the ITO substrate offers new possibilities for charge extraction from photoexcited dyads, and may open a new avenue for development of molecular photovoltaic devices.

■ ASSOCIATED CONTENT

S Supporting Information. ITO surface; conductance and β -values for alkanes on the ITO surface; synthesis of reagents; sample preparation; data analysis and controls for conductance measurements; laser power density measurement; electrochemistry; steady-state spectroscopy; time-resolved fluorescence; and transient absorption. This material is available free of charge via the Internet at <http://pubs.acs.org>.

■ ACKNOWLEDGMENT

This work was supported in part by a NIRT grant of the NSF (0309362). G.K. and the synthesis and spectroscopic measurements were supported as part of the Center for Bio-Inspired Solar Fuel Production, an Energy Frontier Research Center funded by the U.S. Department of Energy, Office of Science, Office of Basic Energy Sciences under Award Number DE-SC0001016. Angle-resolved XPS was carried out by Tim Karcher in the Leroy Eyring Center for Solid State Science. Kaushik Gurunathan assisted us with optics.

■ REFERENCES

- (1) Gust, D.; Moore, T. A. *Science* **1989**, *244*, 35–41.
- (2) Gust, D.; Moore, T. A. *Adv. Photochem.* **1991**, *16*, 1–65.
- (3) Dulic, C.; van der Molen, S. J.; Kudernak, T.; Jonkman, H. T.; De Jong, J. J. D.; Bowden, T. N.; van Esch, J.; Feringa, B. L.; van Wees, B. J. *Phys. Rev. Lett.* **2003**, *91*, 207402-1–4.
- (4) He, J.; Chen, F.; Liddell, P. A.; Andréasson, J.; Straight, S. D.; Gust, D.; Moore, T. A.; Moore, A. L.; Li, J.; Sankey, O. F.; Lindsay, S. M. *Nanotechnology* **2005**, *16*, 695–702.
- (5) Wu, S. W.; Ogawa, N.; Ho, W. *Science* **2006**, *312*, 1362–1365.
- (6) Ward, D. R.; Scott, G. D.; Keane, Z. K.; Halas, N. J.; Natelson, D. *J. Phys. Condens. Matter* **2008**, *20*, 374118.
- (7) Chen, F.; Huang, Z.; Tao, N. *Appl. Phys. Lett.* **2007**, *91*, 162106–162109.
- (8) Kuciauskas, D.; Lin, S.; Seely, G. R.; Moore, A. L.; Moore, T. A.; Gust, D. *J. Phys. Chem.* **1996**, *100*, 15926–15932.
- (9) Xu, B.; Tao, N. J. *Science* **2003**, *301*, 1221–1223.
- (10) Chen, F.; He, J.; Nuckolls, C.; Roberts, T.; Klare, J.; Lindsay, S. M. *Nano Lett.* **2005**, *5*, 503–506.
- (11) Kodis, G.; Liddell, P. A.; Moore, A. L.; Moore, T. A.; Gust, D. *J. Phys. Org. Chem.* **2004**, *17*, 724–734.
- (12) He, J.; Fu, Q.; Lindsay, S. M.; Ciszek, J. W.; Tour, J. M. *J. Am. Chem. Soc.* **2006**, *128*, 14828–14835.

(13) Zhang, J.; Chi, Q.; Kuznetsov, A. M.; Hansen, A. G.; Wackerbarth, H.; Christensen, H. E. M.; Andersen, J. E. T.; Ulstrup, J. *J. Phys. Chem B* **2002**, *106*, 1131–1152.

(14) Gervaldo, M.; Liddell, P. A.; Kodis, G.; Brennan, B. J.; Johnson, C. R.; Bridgewater, J. W.; Moore, A. L.; Moore, T. A.; Gust, D. *Photochem. Photobiol. Sci.* **2010**, *9*, 890–900.